



OPEN

DATA DESCRIPTOR

Chromosome-level genome assembly of the Stoliczka's Asian trident bat (*Aselliscus stoliczkanus*)

Linjing Lan^{1,3}, Xin Zhang^{1,3}, Shanxiu Yang^{1,3}, Lingjie Li²✉ & Xiuguang Mao¹✉

Stoliczka's Asian trident bat (*Aselliscus stoliczkanus*) is a small-bodied species and very sensitive to climate change. Here, we presented a chromosome-level genome assembly of *A. stoliczkanus* by combining Illumina sequencing, Nanopore sequencing and high-throughput chromatin conformation capture (Hi-C) sequencing technology. The genome assembly was 2.18 Gb in size with 98.26% of the genome sequences anchored onto 14 autosomes and two sex chromosomes (X and Y). The quality of the genome assembly is very high with a contig and scaffold N50 of 72.98 and 162 Mb, respectively, Benchmarking Universal Single-Copy Orthologs (BUSCO) score of 96.6%, and the consensus quality value (QV) of 47.44. A total of 20,567 genes were predicted and 98.8% of these genes were functionally annotated. Syntenic blocks between *A. stoliczkanus* and *Homo sapiens*, together with previous comparative cytogenetic studies, provide valuable foundations for further comparative genomic and cytogenetic studies in mammals. The reference-quality genome of *A. stoliczkanus* contributes an important resource for conservative genomics and landscape genomics in predicting adaptation and vulnerability to climate change.

Background & Summary

Stoliczka's Asian trident bat (*Aselliscus stoliczkanus*) is one of the three species in the genus *Aselliscus* (Hipposideridae)¹ and widely distributes in Southeast Asia, including southeastern China, Myanmar, Thailand, Laos, Vietnam, and the Peninsular Malaysia^{2–5}. It is assessed as least concern (LC) by the International Union for Conservation of Nature (IUCN)^{2,5}. However, as a small-bodied species, *A. stoliczkanus* is very sensitive to climate change, in particular to humidity⁶. Thus, although *A. stoliczkanus* has a wide distribution and is listed as LC on the IUCN Red list, previous field surveys of cave bats revealed that the population size of this species has declined rapidly in recent years^{7,8}. So, *A. stoliczkanus* has been recognized as near threatened (NT) on China Species Red List^{9,10}. This species can be regarded as a valuable bio-indicator to climate change, as other bat species^{11,12}. However, up to now, no reference-quality genome has been generated for *A. stoliczkanus*, which is valuable for the assessment of its conservation status and effective protection management^{13,14}.

A. stoliczkanus with diploid chromosome number (2n) of 30 is one of the first bat species whose chromosomes were flow-sorted to be used to generate a whole set of chromosome-specific painting probes¹⁵. As far as we know, chromosome-specific paints of *A. stoliczkanus* have been used in comparative cytogenetic studies on four bat families, including Hipposideridae¹⁶, Rhinolophidae^{15,17,18}, Megadermatidae¹⁹, and Vespertilionidae²⁰. By integrating comparative chromosomal maps between *A. stoliczkanus* (Asto) and *Myotis myotis* (MMY)²¹, as well as between *A. stoliczkanus* and *Homo sapiens* (HSA)¹⁵, conserved syntenies of species from 10 bat families have been generated, which have been used to investigate the chromosomal evolution and predict the ancestral karyotype of Chiroptera^{22,23}. Thus, a reference-quality genome of *A. stoliczkanus* and further whole-genome alignments between *A. stoliczkanus* and the other two species (MMY and HSA) will be very useful to confirm the genome syntenic blocks identified in previous comparative cytogenetic studies.

In this study, we presented a chromosome-level genome assembly for *A. stoliczkanus* using a combination of Illumina short-read sequencing (99.76 Gb), Nanopore long-read sequencing (203.07 Gb) and high-throughput

¹School of Ecological and Environmental Sciences, East China Normal University, Shanghai, 200062, China.

²Department of Histoembryology, Genetics and Developmental Biology, Shanghai Key Laboratory of Reproductive Medicine, Key Laboratory of Cell Differentiation and Apoptosis of Chinese Ministry of Education, Shanghai Jiao Tong University School of Medicine, Shanghai, 200025, China. ³These authors contributed equally: Linjing Lan, Xin Zhang, Shanxiu Yang. ✉e-mail: lingjie@shsmu.edu.cn; xgmao@sklec.ecnu.edu.cn

Library	Reads number	Raw data (Gb)	Clean data (Gb)	Reads N50 (bp)
Illumina	676,766,316	101.52	99.76	/
ONT	12,499,720	204.67	203.07	24,918
Hi-C	1,498,397,190	224.76	222.41	/

Table 1. Statistics of the genome sequencing data for *A. stoliczkanus*.

Feature	Value
Genome assembly statistics	
Estimated genome size (bp)	2,112,045,935
The size of assembly (bp)	2,187,325,338
Contigs number	235
Contigs N50 (bp)	72,975,460
Scaffolds number	191
Scaffolds N50 (bp)	162,004,500
GC content (%)	41.1
Total base on chromosomes (bp)	2,179,935,021
Hi-C loading rates (%)	99.66
Genome assembly evaluation	
Nanopore reads mapping rates (%)	99.96
Illumina reads mapping rates (%)	99.68
Base pair accuracy (QV)	47.44
BUSCO score (%)	96.6

Table 2. Statistics of the genome assembly and genome evaluation for *A. stoliczkanus*.

chromatin conformation capture (Hi-C) sequencing (222.41 Gb) (Table 1). The final genome assembly size was 2.18 Gb with the contig and scaffold N50 of 72.98 Mb and 162 Mb, respectively (Table 2). Consistent with the karyotype reported in previous studies^{15,21}, the final chromosome-level genome assembly includes 14 autosomes, X and Y chromosome (Figs. 1, 2 and Table 3), containing 99.66% of the total genome assembly. Our genome assembly of *A. stoliczkanus* is comparable to other bat genomes (Fig. 3) and can be reliably used in further comparative genomics. In the genome assembly of *A. stoliczkanus* we detected 760.02 Mb (34.75% of the genome) repetitive elements (Table 4). After masking repetitive elements, a total of 20,320 protein-coding genes were predicted and 98.8% of them were functionally annotated (Table 5).

By performing genomic synteny analysis, we validated the results of previous comparative cytogenetic studies between *A. stoliczkanus* and the other two species^{15,21} (Fig. 4 and Table 3). This consistency also supports the high quality of *A. stoliczkanus* genome assembly and annotation generated in this study. Our current genomic resource of *A. stoliczkanus* will be very useful for the assessing of its conservation status and designing effective protection strategies in the future. In addition, syntenic blocks identified between *A. stoliczkanus* and other species will provide valuable foundations for further comparative genomic and cytogenetic studies in bats and also in mammals.

Methods

Sample collection and sequencing. An adult male *A. stoliczkanus* was collected in November 2018 at Xiaogou cave in Yunnan province, China (25°03'16.7"N, 103°22'52.5"E). Bat was euthanized by cervical dislocation and four tissues (muscle, heart, brain, and liver) were sampled with RNase-free tubes. All tissues were frozen immediately in liquid nitrogen and then were stored in a -80 °C freezer. Sampling and tissue collection procedures were approved by the National Animal Research Authority, East China Normal University (approval ID bf20190301).

For genome sequencing, genomic DNA extracted from muscle with DNeasy kits (Qiagen) was used to construct three different sequencing libraries. First, Nanopore long read library (DNA fragment >20 kb) was constructed with the SQK-LSK109 kit (Oxford Nanopore Technologies, UK) and sequenced on a PromethION sequencer (Oxford Nanopore). The quality of Nanopore reads was assessed using Nanoplot v1.40.2²⁴ and results have been shown in supplementary Table S1. Then reads were further trimmed by Nanofilt v2.8.0²⁴ with default parameters. Second, for genome survey and error correction of Nanopore data, Illumina short read library (DNA fragment ~350 bp) was constructed with the NEBNext Ultra DNA library Pre-Kit and sequenced on the Illumina Novaseq. 6000 platform (pair-end 150 bp). Illumina short reads were assessed and trimmed by fastp v0.23.2²⁵ (-q 20 -w 5 -u 40 -n 5). Third, to generate a chromosome-level genome, we created the Hi-C library with the Truseq Nano DNA library Kit and the restriction endonuclease DpnII following procedures described previously²⁶ and sequenced it on the Illumina Hiseq platform (pair-end 150 bp). Hi-C reads were also processed by fastp v0.23.2²⁵.

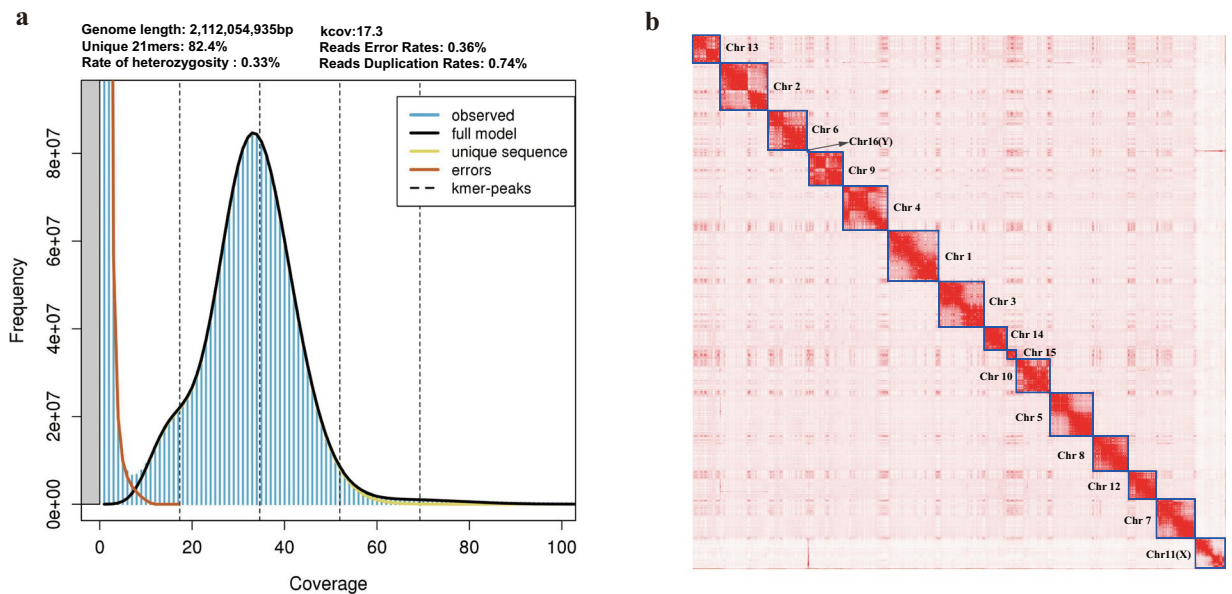


Fig. 1 (a) Genomescope profile for 21-mers based on Illumina short-reads. (b) Hi-C contact map for the genome assembly.

For transcriptome sequencing, the total RNA of each tissue (heart, brain and liver) was extracted using TRIzol (Life Technologies Corp., Carlsbad, CA, USA). A total of three RNA sequencing libraries were constructed using NEBNext® UltraTM RNA Library Prep Kit for Illumina® (NEB, USA) and sequenced on the Illumina HiSeq X Ten platform (paired-end 150 bp). RNA-seq reads were trimmed using TRIMMOMATIC v0.38²⁷ with default parameters.

Genome assembly. Jellyfish v2.2.10²⁸ was used to construct the k-mer count histogram ($k=21$) based on 99.76 Gb clean short read data. Then, the genome size, heterozygosity and percentage of repeat content were estimated using GenomeScope v2.0²⁹. Genomic contig assembly was performed based on 203.07 Gb Nanopore long reads using NextDenovo³⁰ software (<https://github.com/nextomics/nextdenovo>). Then Nextpolish v1.4.1³¹ was applied to polish the assembly with both Nanopore long reads and Illumina short reads. Redundant contigs were removed using Purge_Dups v1.2.5³² with default settings. A total of 222.41 Gb clean Hi-C reads were then mapped to the contig assembly using Juicer v1.6³³ and chromosome construction was conducted using the 3D-DNA pipeline³⁴ with default settings. We further used Juicebox Assembly Tools³⁵ to manually correct the chromatin contact matrix and built the Hi-C interaction heatmap. The final genome assembly was generated by 3D-DNA post-review pipeline based on the corrected assembly file above.

To evaluate the quality of the genome assembly, we first assessed its integrity using Benchmarking Universal Single-Copy Orthologs (BUSCO v5.2.2)³⁶ with a database of mammals (mammalia_odb10). Second, the Nanopore long reads and Illumina short reads were mapped to the genome assembly using minimap2 v2.24-r1122³⁷ and bwa v0.7.17-r1188³⁸ with default parameters, respectively. We then estimated the mapping rates using SAMtools v1.16.1³⁹. Third, the accuracy of our genome assembly was assessed by calculating the consensus quality (QV) using MERQURY v1.3⁴⁰ based on Illumina short reads and k-mers.

Identification of sex chromosomes. We identified the X chromosome of *A. stoliczkanus* by aligning its genome assembly against the genome of *R. ferrumequinum* (NCBI accession number: GCF_004115265.2) whose X chromosome had been identified⁴¹. Y chromosome of *A. stoliczkanus* was identified by performing blastn searches with Y-linked genes in the mammals (*USP9Y* and *UTY*)⁴².

Repeat annotation. We annotated the repeat sequences in the *A. stoliczkanus* genome using both de novo and homology-based prediction methods. A de novo repeat library was first created using RepeatModeler (<https://github.com/Dfam-consortium/RepeatModeler>) (the ‘-LTRStruct’ option), which was merged with the bat repeat libraries⁴³, Repbase (<http://www.girinst.org/repbase>) and Dram database to generate a final custom repeat library. RepeatMasker v4.1.2⁴⁴ was then used to perform repeat sequence annotation with the custom repeat library. A total of 760.02 Mb (34.75% of the genome) repetitive elements were identified, of which 33.12% was transposable elements (TEs), including LINE (19.78%), LTR (5.93%), SINE (2.34%), DNA transposons (4.89%), Rolling-circles (0.13%) and unclassified TEs (0.13%) (Table 4).

Gene annotation. We used three methods to predict protein-coding genes, including ab initio prediction, transcriptome-based prediction and homology-based prediction. The BRAKER2 v2.5.2 pipeline⁴⁵ was applied to perform ab initio prediction using de novo, homology-based protein and RNA-Seq evidence. For transcriptome-based prediction, a total of 21.3 Gb RNA-seq reads from four tissues were mapped to the

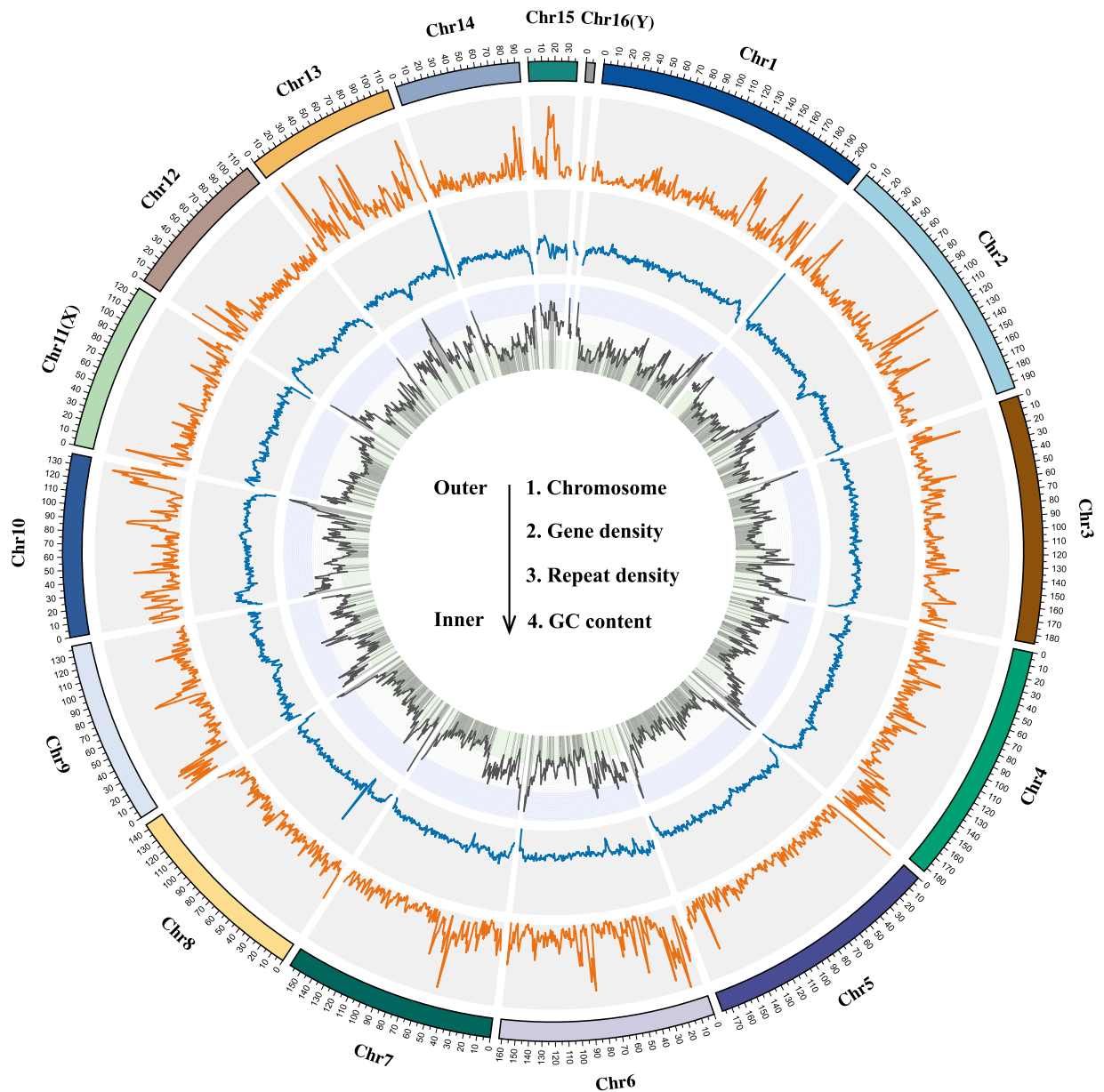


Fig. 2 Circos showing the genomic structure of *A. stoliczkanus* including chromosome, gene density, repeat density, and GC content (%) from the outer circle to inner one.

genome using HISAT2 v2.2.1⁴⁶ with default parameters and the transcriptome was assembled using STRINGTIE v2.2.1⁴⁷. The open reading frames (ORFs) were predicted by TransDecoder v5.5.0 (<https://github.com/TransDecoder/TransDecoder/>). Homology-based prediction was performed using GEMOMA v1.9.0^{48,49} based on protein sequences of 11 species including six bats (*Rousettus aegyptiacus*, *Rhinolophus ferrumequinum*, *Pipistrellus kuhlii*, *Phyllostomus discolor*, *Myotis myotis*, and *Molossus molossus*) and five other mammals (*Felis catus*, *Bos taurus*, *Sus scrofa*, *Mus musculus*, and *Homo sapiens*). Then, we used EVIDENCEModeler v2.0.0⁵⁰ to combine genes predicted by the three methods with a weighted consensus (ABINITIO_PREDICTION AUGUSTUS 1, TRANSCRIPT Cufflinks 12, OTHER_PREDICTION GeMoMa 10, OTHER_PREDICTION transdecoder 12). Finally, two rounds of PASA v2.4.1⁵¹ were conducted to update the EVM result using the transcriptome de novo assembled by Trinity v2.13.2⁵² under the default settings. We performed functional annotation by searching sequences of protein-coding genes against the Uniprot database and nonredundant protein sequence database (NR) using DIAMOND (blastp -e 1e-5)⁵³, and the eggNOG database using EggNOG-mapper⁵⁴. In addition, INTERPROSCAN⁵⁵ (-appl Pfam -iprlookup -goterms) was employed to obtain protein domains and motifs and gene ontology (GO).

Genome synteny. Genomic synteny analyses were performed between *A. stoliczkanus* and two other species (*M. myotis* and *H. sapiens*). We first conducted the pairwise alignment of these chromosome-level genomes using

Chromosome ID	Chromosome ID in previous study ¹⁵	Chromosome Length (bp)
Chr1	Chr1	207,901,853
Chr2	Chr3	194,675,023
Chr3	Chr4	186,534,500
Chr4	Chr2	183,023,020
Chr5	Chr7	177,415,154
Chr6	Chr5	162,004,500
Chr7	Chr6	158,905,207
Chr8	Chr8	143,714,873
Chr9	Chr9	137,972,201
Chr10	Chr11	137,439,702
Chr11(X)	X	126,483,028
Chr12	Chr12	113,898,000
Chr13	Chr10	113,190,041
Chr14	Chr13	93,423,647
Chr15	Chr14	36,716,714
Chr16(Y)	Y	6,637,558

Table 3. The length of each chromosome in the genome assembly of *A. stoliczkanus*.

Type of elements	Number of elements	Length (bp)	Percentage of genome (%)
SINEs	357,754	51,157,424	2.34
LINEs	829,135	432,550,674	19.78
LTR elements	428,008	129,647,761	5.93
DNA transposons	591,882	106,858,154	4.89
Rolling-circles	16,062	1,164,855	0.05
Unclassified	17,137	2,842,690	0.13
Total interspersed repeats	2,239,978	724,221,558	33.12
Satellites	8,556	1,279,207	0.06
Simple repeats	698,500	29,828,252	1.36
Low complexity	93,923	4,693,480	0.21
Total tandem repeats	800,979	35,800,939	1.63
Total	3,040,957	760,022,497	34.75

Table 4. Summary of repetitive elements in the genome assembly of *A. stoliczkanus*.

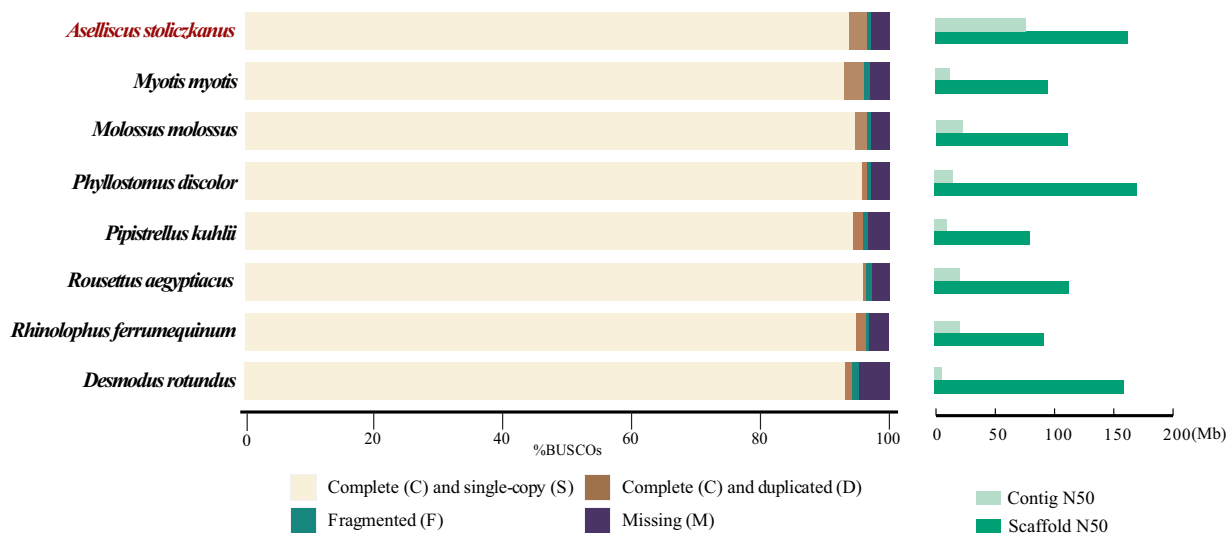


Fig. 3 The contiguity of the genome assembly revealed by Benchmarking Universal Single-Copy Orthologs (BUSCO) score and N50 of contig and scaffold. Genome assembly of *Aselliscus stoliczkanus* was shown in red.

Item	Number	Average length (bp)
Gene	20,567	45,892.69
Exon	422,449	279.57
CDS	403,817	166.47
Database	Number	Percentage (%)
Pfam	17,687	86
SwissProt	19,253	93.61
NR	18,068	87.85
eggNOG	19,776	96.15
All	20,320	98.8

Table 5. Summary of gene structures and function in *A. stoliczkanus*.

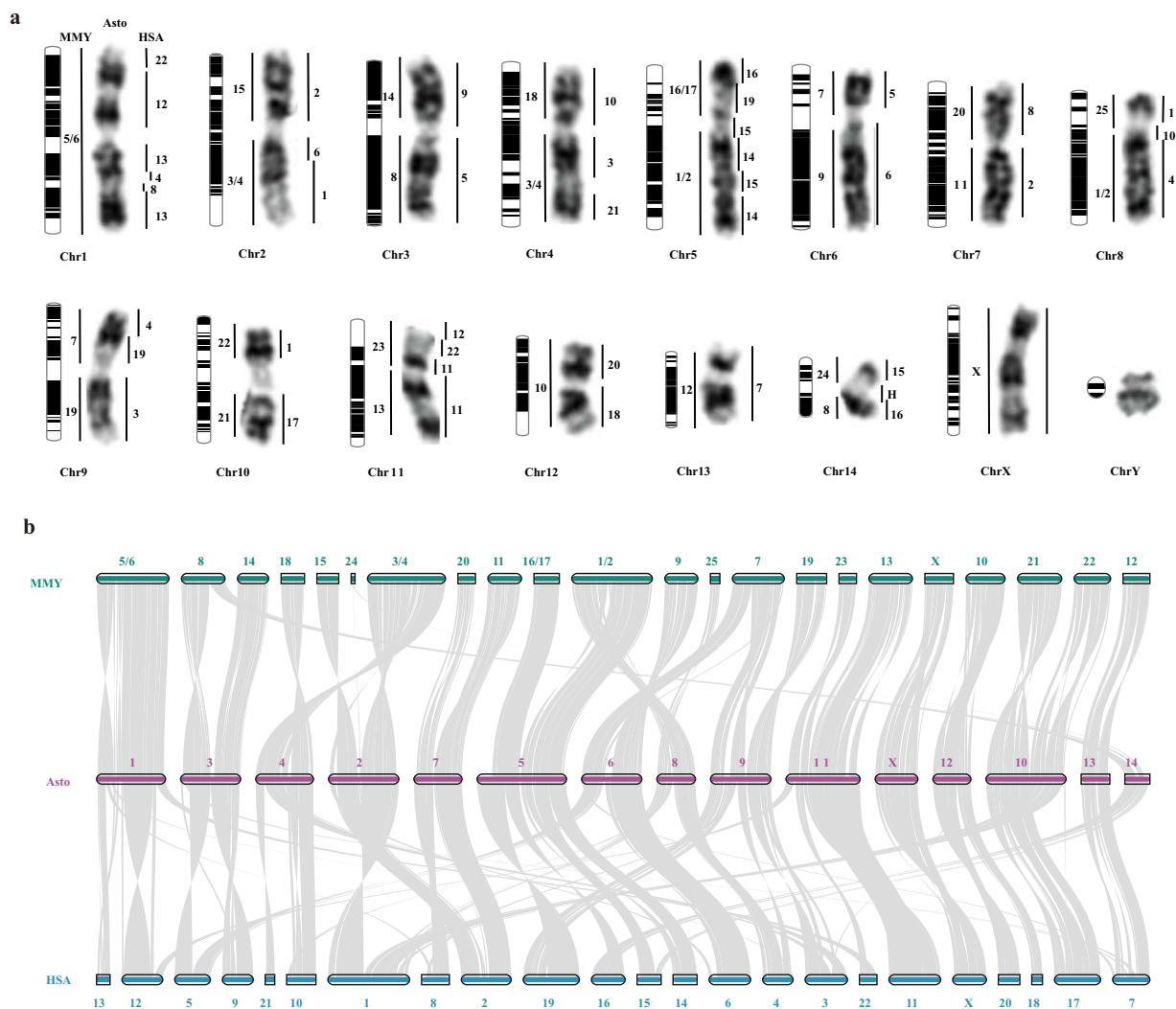


Fig. 4 (a) G-banded karyotype of *A. stoliczkanus* with syntenic blocks between *A. stoliczkanus* (Asto) and two other species (*Myotis myotis*: MMY; *Homo sapiens*: HSA), identified in previous comparative cytogenetic studies¹⁵. The capital letter “H” in chromosome 14 represents heterochromatin. The diagram for each chromosome is also shown on the left and the black color in the diagram represents the regions in which the GC content of a 1-Mb window is lower than the average GC content of the chromosome. (b) Genomic synteny and collinearity among Asto, MMY and HSA. Chromosomes in the genome assembly of MMY were numbered on the basis of previously published flow karyotype of this species²¹.

LAST software v1410⁵⁶, then we identified and visualized the syntenic blocks using MCscan (python version) with default parameters. High collinearity was observed across the three species (Fig. 4b) and syntenic blocks identified here could be used to validate the results of previous comparative cytogenetic studies.

Data Records

All raw sequencing data that were used for genome assembly and annotation have been deposited into the National Center for Biotechnology Information (NCBI) with accession number SRR25459631⁵⁷ and SRR25476260⁵⁸ for Illumina sequencing data, SRR25470059⁵⁹ and SRR25470058⁶⁰ for Nanopore sequencing data, SRR25490035⁶¹ for Hi-C sequencing data, SRR25461847⁶², SRR25461853⁶³, and SRR25461918⁶⁴ for transcriptome Illumina sequencing data. The final genome assembly and gene annotation results have been deposited in Figshare⁶⁵ and in the GenBank database of NCBI with accession number JAWWOG000000000⁶⁶.

Technical Validation

High quality of the genome assembly of *A. stoliczkanus* was supported by multiple evaluation methods (BUSCO score: 96.6%; QV value: 47.44; mapping rates of Illumina short reads and Nanopore long reads: 99.68% and 99.96%, Table 2). In addition, the final assembled chromosome-level genome (99.66% of the total genome) contained the same number of chromosomes with the karyotype reported previously. Finally, highly homologous genomic segments between *A. stoliczkanus* and two other species (*M. myotis* and *H. sapiens*) revealed by genomic synteny analysis also supported the high quality of the genome assembly and annotation of *A. stoliczkanus*.

Code availability

All commands and pipelines used in the data processing were all executed according to the manuals and protocols of the corresponding bioinformatics software. If no detailed parameters were provided, default parameters were used. The version of the software has been specified in the Methods section. No custom programming or coding was used.

Received: 9 August 2023; Accepted: 8 December 2023;

Published online: 15 December 2023

References

- Dobson, G. E. On a new genus and species of Rhinolophidae, with description of a new species of *Vesperugo*, and notes on some other species of insectivorous bats from Persia. *J. Asiatic Soc. Bengal.* **40**, 455–461 (1871).
- Bates, P., Bumrungsri, S., Francis, C., Csorba, G. & Furey, N. *Aselliscus stoliczkanus*. *The IUCN Red List of Threatened Species* 2008, e.T2155A9300617 (2008).
- Francis, C. M. A field guide to the mammals of South-East Asia. *Mammalia* **73**, 78–80 (2009).
- Zhang, Z. *et al.* Variation in *Aselliscus stoliczkanus* based on morphology and molecular sequence data, with a new record of the genus *Aselliscus* in China. *J. Mammal.* **97**, 1718–1727 (2016).
- Tu, V., Görföl, T., Furey, N. & Csorba, G. *Aselliscus stoliczkanus*. *The IUCN Red List of Threatened Species* 2022, e.T214518902A21976509 (2022).
- Liu, Y., Wang, Y., Zhang, Z., Bu, Y. & Niu, H. Roost selection and ecology of *Stoliczka's* trident bat, *Aselliscus stoliczkanus* (Hipposideridae, Chiroptera) in China. *Mamm. Biol.* **95**, 143–149 (2019).
- Zhang, L., Jones, G. & Zhang, J. Recent surveys of bats (Mammalia: Chiroptera) from China. *Acta Chiropterol.* **11**, 71–88 (2009).
- Bu, Y. *et al.* Geographical distribution, roost selection, and conservation state of cave-dwelling bats in China. *Mammalia* **79**, 409–417 (2015).
- Wang, S. & Xie, Y. *China Species Red List* (Higher Education Press, 2004).
- Jiang, Z. *China's Red List of Biodiversity: Vertebrates* (Science Press, 2021).
- Jones, G., Jacobs, D. S., Kunz, T. H., Willig, M. R. & Racey, P. A. Carpe noctem: the importance of bats as bioindicators. *Endanger Species Res.* **8**, 93–115 (2009).
- Festa, F. *et al.* Bat responses to climate change: a systematic review. *Biol. Rev.* **98**, 19–33 (2023).
- Formenti, G. *et al.* The era of reference genomes in conservation genomics. *Trends Ecol. Evol.* **37**, 197–202 (2022).
- Wilder, A. P. *et al.* The contribution of historical processes to contemporary extinction risk in placental mammals. *Science* **380**, eabn5856 (2023).
- Mao, X. *et al.* Karyotype evolution in *Rhinolophus* bats (Rhinolophidae, Chiroptera) illuminated by cross-species chromosome painting and G-banding comparison. *Chromosome Res.* **15**, 835–848 (2007).
- Mao, X. *et al.* Karyotypic evolution in family Hipposideridae (Chiroptera, Mammalia) revealed by comparative chromosome painting, G- and C-banding. *Zool. Res.* **31**, 453 (2010).
- Volleth, M. *et al.* Comparative chromosomal studies in *Rhinolophus formosae* and *R. luctus* from China and Vietnam: elevation of *R. l. lanosus* to species rank. *Acta Chiropterol.* **19**, 41–50 (2017).
- Volleth, M. *et al.* Cytogenetic investigations in Bornean Rhinolophoidea revealed cryptic diversity in *Rhinolophus sedulus* entailing classification of Peninsular Malaysia specimens as a new species. *Acta Chiropterol.* **23**, 1–20 (2021).
- Volleth, M. *et al.* Cytogenetic analyses detect cryptic diversity in *Megaderma spasma* from Malaysia. *Acta Chiropterol.* **23**, 271–284 (2022).
- Kulemzina, A. I. *et al.* Comparative chromosome painting of four Siberian Vespertilionidae species with *Aselliscus stoliczkanus* and human probes. *Cytogenet. Genome Res.* **134**, 200–205 (2011).
- Ao, L. *et al.* Karyotypic evolution and phylogenetic relationships in the order Chiroptera as revealed by G-banding comparison and chromosome painting. *Chromosome Res.* **15**, 257–268 (2007).
- Mao, X. *et al.* Comparative cytogenetics of bats (Chiroptera): The prevalence of Robertsonian translocations limits the power of chromosomal characters in resolving interfamily phylogenetic relationships. *Chromosome Res.* **16**, 155–170 (2008).
- Sotero-Caio, C. G., Baker, R. J. & Volleth, M. Chromosomal evolution in Chiroptera. *Genes* **8**, 272 (2017).
- De Coster, W., D'hert, S., Schultz, D. T., Cruts, M. & Van Broeckhoven, C. NanoPack: visualizing and processing long-read sequencing data. *Bioinformatics* **34**, 2666–2669 (2018).
- Chen, S., Zhou, Y., Chen, Y. & Gu, J. fastp: an ultra-fast all-in-one FASTQ preprocessor. *Bioinformatics* **34**, i884–i890 (2018).
- Belton, J. M. *et al.* Hi-C: A comprehensive technique to capture the conformation of genomes. *Methods* **58**, 268–276 (2012).
- Bolger, A. M., Lohse, M. & Usadel, B. Trimmomatic: a flexible trimmer for Illumina sequence data. *Bioinformatics* **30**, 2114–2120 (2014).
- Marçais, G. & Kingsford, C. A fast, lock-free approach for efficient parallel counting of occurrences of k-mers. *Bioinformatics* **27**, 764–770 (2011).
- Vurtture, G. W. *et al.* GenomeScope: fast reference-free genome profiling from short reads. *Bioinformatics* **33**, 2202–2204 (2017).

30. Hu, J. *et al.* An efficient error correction and accurate assembly tool for noisy long reads. 2023.03.09.531669 Preprint at <https://doi.org/10.1101/2023.03.09.531669> (2023).
31. Hu, J., Fan, J., Sun, Z. & Liu, S. NextPolish: a fast and efficient genome polishing tool for long-read assembly. *Bioinformatics* **36**, 2253–2255 (2020).
32. Guan, D. *et al.* Identifying and removing haplotypic duplication in primary genome assemblies. *Bioinformatics* **36**, 2896–2898 (2020).
33. Durand, N. C. *et al.* Juicer provides a one-click system for analyzing loop-resolution Hi-C experiments. *Cell Syst.* **3**, 95–98 (2016).
34. Dudchenko, O. *et al.* De novo assembly of the *Aedes aegypti* genome using Hi-C yields chromosome-length scaffolds. *Science* **356**, 92–95 (2017).
35. Durand, N. C. *et al.* Juicebox provides a visualization system for Hi-C contact maps with unlimited zoom. *Cell Syst.* **3**, 99–101 (2016).
36. Manni, M., Berkeley, M. R., Seppy, M., Simão, F. A. & Zdobnov, E. M. BUSCO update: novel and streamlined workflows along with broader and deeper phylogenetic coverage for scoring of eukaryotic, prokaryotic, and viral genomes. *Mol. Biol. Evol.* **38**, 4647–4654 (2021).
37. Li, H. Minimap2: pairwise alignment for nucleotide sequences. *Bioinformatics* **34**, 3094–3100 (2018).
38. Li, H. Aligning sequence reads, clone sequences and assembly contigs with BWA-MEM. *Genomics*. **0**, 1–3 (2013).
39. Danecek, P. *et al.* Twelve years of SAMtools and BCFtools. *GigaScience* **10**, giab008 (2021).
40. Rhie, A., Walenz, B. P., Koren, S. & Phillippy, A. M. Merqury: reference-free quality, completeness, and phasing assessment for genome assemblies. *Genome Biol.* **21**, 245 (2020).
41. Jebb, D. *et al.* Six reference-quality genomes reveal evolution of bat adaptations. *Nature* **583**, 578–584 (2020).
42. Godfrey, A. K. *et al.* Quantitative analysis of Y-Chromosome gene expression across 36 human tissues. *Genome Res.* **30**, 860–873 (2020).
43. Scheben, A. *et al.* Long-read sequencing reveals rapid evolution of immunity- and cancer-related genes in bats. *Genome Biol. Evol.* **15**, evad148 (2023).
44. Chen, N. Using RepeatMasker to identify repetitive elements in genomic sequences. *Curr. Protoc. Bioinformatics* **5**, 4.10.1–4.10.14 (2004).
45. Bruna, T., Hoff, K. J., Lomsadze, A., Stanke, M. & Borodovsky, M. BRAKER2: automatic eukaryotic genome annotation with GeneMark-EP plus and AUGUSTUS supported by a protein database. *Nar Genom. Bioinform.* **3**, lqaa108 (2020).
46. Kim, D., Paggi, J. M., Park, C., Bennett, C. & Salzberg, S. L. Graph-based genome alignment and genotyping with HISAT2 and HISAT-genotype. *Nat. Biotechnol.* **37**, 907–915 (2019).
47. Pertea, M., Kim, D., Pertea, G. M., Leek, J. T. & Salzberg, S. L. Transcript-level expression analysis of RNA-seq experiments with HISAT, StringTie and Ballgown. *Nat. Protoc.* **11**, 1650–1667 (2016).
48. Keilwagen, J. *et al.* Using intron position conservation for homology-based gene prediction. *Nucleic Acids Res.* **44**, 89–89 (2016).
49. Keilwagen, J., Hartung, F., Paulini, M., Twardziok, S. O. & Grau, J. Combining RNA-seq data and homology-based gene prediction for plants, animals and fungi. *BMC Bioinformatics* **19**, 189 (2018).
50. Haas, B. J. *et al.* Automated eukaryotic gene structure annotation using EVidenceModeler and the Program to Assemble Spliced Alignments. *Genome Biol.* **9**, R7 (2008).
51. Haas, B. J. *et al.* Improving the *Arabidopsis* genome annotation using maximal transcript alignment assemblies. *Nucleic Acids Res.* **31**, 5654–5666 (2003).
52. Grabherr, M. G. *et al.* Full-length transcriptome assembly from RNA-Seq data without a reference genome. *Nat. Biotechnol.* **29**, 644–652 (2011).
53. Buchfink, B., Xie, C. & Huson, D. H. Fast and sensitive protein alignment using DIAMOND. *Nat. Methods* **12**, 59–60 (2015).
54. Cantalapiedra, C. P., Hernández-Plaza, A., Letunic, I., Bork, P. & Huerta-Cepas, J. eggNOG-mapper v2: functional annotation, orthology assignments, and domain prediction at the metagenomic scale. *Mol. Biol. Evol.* **38**, 5825–5829 (2021).
55. Jones, P. *et al.* InterProScan 5: genome-scale protein function classification. *Bioinformatics* **30**, 1236–1240 (2014).
56. Kielbasa, S., Wan, R., Sato, K., Horton, P. & Frith, M. Adaptive seeds tame genomic sequence comparison. *Genome Res.* **21**, 487–93 (2011).
57. NCBI Sequence Read Archive <https://identifiers.org/ncbi/insdc.sra:SRR25459631> (2023).
58. NCBI Sequence Read Archive <https://identifiers.org/ncbi/insdc.sra:SRR25476260> (2023).
59. NCBI Sequence Read Archive <https://identifiers.org/ncbi/insdc.sra:SRR25470059> (2023).
60. NCBI Sequence Read Archive <https://identifiers.org/ncbi/insdc.sra:SRR25470058> (2023).
61. NCBI Sequence Read Archive <https://identifiers.org/ncbi/insdc.sra:SRR25490035> (2023).
62. NCBI Sequence Read Archive <https://identifiers.org/ncbi/insdc.sra:SRR25461847> (2023).
63. NCBI Sequence Read Archive <https://identifiers.org/ncbi/insdc.sra:SRR25461853> (2023).
64. NCBI Sequence Read Archive <https://identifiers.org/ncbi/insdc.sra:SRR25461918> (2023).
65. Lan, L. Genome assembly and annotation of *Aselliscus stoliczkanus*. *Figshare* <https://doi.org/10.6084/m9.figshare.23902812.v2> (2023).
66. Genome assembly of *Aselliscus stoliczkanus*. *GenBank* <https://identifiers.org/ncbi/insdc:JAWWOG000000000> (2023).

Acknowledgements

We thank Sun Haijian and Wang Jiaying for their help in field work. This work was supported by Program for Oriental Scholars of Shanghai Universities (to Li L.J.), Shanghai Frontiers Science Center of Cellular Homeostasis and Human Diseases (to Li L.J.).

Author contributions

Mao X.G. and Li L.J. conceived and supervised the project. Lan L.J., Zhang X. and Yang S.X. analyzed data. Mao X.G. wrote the manuscript with the input of Lan L.J. All authors edited the manuscript and approved the final version of the manuscript.

Competing interests

The authors declare no competing interests.

Additional information

Supplementary information The online version contains supplementary material available at <https://doi.org/10.1038/s41597-023-02838-0>.

Correspondence and requests for materials should be addressed to L.L. or X.M.

Reprints and permissions information is available at www.nature.com/reprints.

Publisher's note Springer Nature remains neutral with regard to jurisdictional claims in published maps and institutional affiliations.



Open Access This article is licensed under a Creative Commons Attribution 4.0 International License, which permits use, sharing, adaptation, distribution and reproduction in any medium or format, as long as you give appropriate credit to the original author(s) and the source, provide a link to the Creative Commons licence, and indicate if changes were made. The images or other third party material in this article are included in the article's Creative Commons licence, unless indicated otherwise in a credit line to the material. If material is not included in the article's Creative Commons licence and your intended use is not permitted by statutory regulation or exceeds the permitted use, you will need to obtain permission directly from the copyright holder. To view a copy of this licence, visit <http://creativecommons.org/licenses/by/4.0/>.

© The Author(s) 2023